JFBE 6(1): 8-17, 2023

Journal of Food and Bioprocess Engineering

Journal homepage: https://jfabe.ut.ac.ir

Original research

Development and performance evaluation of small-scale low-viscous juice continuous pasteurizer

Julia Kigozi*, Emmanuel Baidhe, Hussein Kivumbi Balimunsi

Department of Agricultural & Biosystems Engineering, Makerere University P. O. Box 7062, Kampala, Uganda

A B S T R A C T

Pasteurization is regarded as a critical unit operation in the juice processing chain because it extends the juice's shelf life. This study aimed to design, construct and assess the performance of the small-scale low-viscous juice continuous pasteurizer. The pasteurizer is equipped with three shell and tube heat exchangers (STHE) that operate on a counter-current flow system. During operation, raw juice is preheated in the regeneration section before being heated in the heating section to a specified pasteurization temperature. The juice is then held at pasteurization temperature in holding tubes for a specific period before being cooled in the regeneration and cooling section. The performance was evaluated by determining the maximum hot water temperature attainable, product pasteurization temperature and throughput at various pumping speeds of the product. With an initial heating time of 23 minutes, all product pump speeds over 792 rpm can yield a regeneration efficiency of about 50% with a throughput capacity of about 600 L/h. An automated control system can be used to adjust the pasteurizing temperatures. This enables effective use with a wide range of food products with pasteurization temperatures ranging from 72°C to 88°C under High-Temperature-Short-Time (HTST) processing. The logarithmic and quadratic polynomial models were found to be suitable for predicting throughput capacity and pasteurization temperature, respectively. The results from the validation showed R^2 values of 97.52% and 99.28% for throughput capacity and pasteurization temperature, respectively. Juice pump speed did not affect the regeneration efficiency ($p < 0.05$). The pasteurizer is suitable for low-viscous food products.

Keywords: Pasteurization; Low-viscous juice; Energy recovery; Continuous pasteurizer

Received 05 August 2022; Revised 15 January 2023; Accepted 02 March 2023

1. Introduction

Agriculture alone contributes about 26% of Uganda's total Gross Domestic Product (GDP) (Deloitte, 2016), while generating employment for close to 70% of the country's working population (Kuteesa et al., 2018). Thus, agriculture has attracted great promotion and funding for development through the Government of Uganda and its partners, as witnessed in the horticultural industry (Ankwasa, 2018). Majority of the horticultural fruit produced is freshly consumed locally, with only a small amount being exported. According to Wakholi et al. (2015), the fruit consumption rate in Uganda still lies below the national level recommendation of 80g per capita per day. The unconsumed fruit usually deteriorates in quality, contributing to post-harvest losses (PHLs). PHLs are caused by lack of relevant processing technologies, limited access to information, and insufficient credit to purchase the appropriate facilities (Kumari & Kumar, 2018; Rahiel et al., 2018). High PHLs have a big impact on farmers' incomes and the country's food security. As a result, reduction of PHLs is a good way to improve food security and overall farmers' incomes (Kikulwe et al., 2018; Kughur et al., 2015).

Although juices are highly perishable, farmers and fruit dealers are processing their fruit into juice to reduce the PHLs. Juice production involves the following steps: washing, culling, juice extraction, pasteurization using the thermal treatment, filling, and storage. Thermal processing is considered a critical unit operation in juice processing as it extends the juice shelf life by reducing microbiological load and enzymatic activity of the food (Sarkar, 2015). Thermal processing entails heating the juice to a specific temperature in order to reduce microbial load and ensure enzyme

*Corresponding author.
E-mail address: jbulyakigozi@yahoo.com (J. Kigozi).
https://doi.org/10.22059/jfabe.2023.346742.1124

inactivation. More specifically, food is heated to relative temperatures (<100°C), a process called pasteurization.

Pasteurization world over is carried out using either batch or continuous pasteurizers. In Uganda, some effective efforts have been made to reduce losses associated with deterioration of fruit pulp and juice quality. Several batch pasteurizers have been developed and adopted locally. The batch system, however, processes a specific volume of product per unit time. It is therefore very inconvenient for a processor with large volumes because they must constantly empty and refill the vat. Large amounts of juice require a lot of resources in terms of labor, time, and energy to process (Amit et al., 2017). As a result, juice and pulp processors are unable to increase production. Processors who choose to import continuous pasteurizers from Europe and Asia face high importation costs resulting from high taxes. They are also faced with maintenance challenges because these products come with unique technology that can only be serviced by expert technicians who must also be outsourced. There is need to develop continuous pasteurizers in Uganda so that juice processors can increase the volume of juice produced per unit time while using less labor and energy, lowering the overall cost of operation (Widiatmo & Hendrarsakti, 2018). This study aimed to design, construct and assess the performance of the small-scale low-viscous juice continuous pasteurizer.

This study aimed to enhance Uganda's small-scale processors' processing capabilities. There is no doubt that some initiatives have been successful, particularly in Uganda where pasteurization technology has replaced the crude source pan-based pasteurization among small-scale processors. For instance, batch pasteurizers were developed in Uganda by Ahumuza et al. (2017) and Ninshaba (2015). Despite their production efficiency, the developed batch pasteurizers are associated with a lot of drudgery (labor, time, and energy). For instance, all energy used to heat the product during pasteurization is lost in the process of product cooling, a high labor force is required to effectively manage the pasteurization process in case of large production, thus increasing the overall energy requirement during production. Moreover, the production rate of 92-194 L/h as established for the batch pasteurizer developed by Ahumuza et al. (2017) still limits the production expansion requirements for an average small-scale daily processor production needs of about 360L (Uganda Investment Authority, n.d.). These drawbacks are well addressed with the use of continuous pasteurization systems (Baidhe et al., 2022). However, no research on the development of continuous pasteurizers specifically designed for small-scale processors in Uganda has been documented. In this study, an energy recovery system was incorporated into the design for this study to improve the production's overall energy consumption. This study acknowledges the numerous continuous pasteurizers imported by well-established processing firms. Despite having similar working principles, the present work focused on developing a more user-friendly and tailor-made design appropriate for use in Uganda. Compared to imported designs that come with unique automation needs, the design in the present work involves limited automation yet with increased processor production capacity. The design used in this study is not anchored on a particular customized computer program, without which the machine would not operate as it does for the other imported machines.

2. Material and Methods

2.1. Design of continuous pasteurizer components

2.1.1. Design of raw juice tank

The dimensions for the 100 L tank were calculated using Eq. (1). A tank of capacity 100 L (0.1 m^3) would equitably support the production of a small-scale business with a target of about 100 dozens of 300 mL bottles per day (estimated at 360 L per day) (Uganda Investment Authority, n.d.), since it only holds the raw juice during production.

$$Volume = \pi r^2 h \quad (1)$$

where r and h are the radius (m) and height (m) of the tank, respectively.

2.1.2. Heat exchanger design

The Log Mean Temperature Difference (LMTD) method was used in the design of heat exchangers because it is very convenient. The LMTD serves as an equivalent mean temperature difference between the two fluids for the entire heat exchanger (Marwa, 2021). The heat exchangers' design included determining the heat load required for the process and maximizing the transfer of heat load between the fluids. The design took the following procedure:

(a) Determination of heat load [$\dot{q}$]

The ratio of outlet temperature gap to inlet temperature (G) was instrumental in the estimation of temperatures for both the cold and hot fluids that can allow effective heat transfer. G given by Eq. (2) has a range of values between +1 and -1. The heat exchanger must function under temperature approach circumstances, where the cold stream final temperature is lower than the hot fluid output temperature, for effective heat transfer. Temperature approach is represented by a positive G value, whereas temperature cross is represented by a negative G value (Vengateson, 2010).

$$G = \frac{T_{out} - t_{out}}{T_{in} - t_{in}} \quad (2)$$

where T_{in} and T_{out} - the hot side fluid inlet and outlet temperatures respectively (°C), t_{in} and t_{out} - the cold side fluid inlet and outlet temperatures respectively (°C).

Leaving aside the negligible heat losses to the atmosphere, the heat load is the heat lost by one fluid on one side of the heat exchanger and gained by another on the other. The heat load ($\dot{q}$) for the heat exchanger was determined using Eq. (3).

$$\dot{q} = \dot{m} C \Delta T \quad (3)$$

where C - the fluid specific heat capacity (J/kgK), m - the fluid mass flow rate (kg/s), ΔT - the temperature difference (°C).

(b) Estimation of log mean temperature difference (LMTD) [ΔT_l]

The LMTD was determined using Eq. (4) (Chavhan et al., 2016).

$$\Delta T_1 = \frac{F(\Delta T_a - \Delta T_b)}{In\left(\frac{\Delta T_a}{\Delta T_b}\right)} \quad (4)$$

where ΔT_a - the temperature difference between the inlet temperature for the shell fluid and exit temperature for the tube fluid and ΔT_b - the temperature difference between the exit temperature of the shell fluid and the inlet temperature of tube fluid, F – the correction factor.

The correction factor (F) was estimated from correction factor charts using the values of thermal effectiveness (P) and heat capacity ratio (R) determined by Eq. (5) and (6), respectively (Lebele-Alawa & Ohia, 2014).

$$P = \frac{t_2 - t_1}{T_1 - t_1} \quad (5)$$

$$R = \frac{T_1 - T_2}{t_2 - t_1} \quad (6)$$

where T_1 and T_2 are the entry and exit temperatures at for the shell fluid, t_1 and t_2 are the entry and exit temperatures for the tube fluid.

(c) Estimation of the heat transfer area [A_H]

The heat transfer area (A_H) was determined by the heat load, LMTD, and the overall heat transfer coefficient (Qian et al., 2021) using Eq. (7).

$$A_H = \frac{\dot{q}}{U_o \times \Delta T_1} \quad (7)$$

where U_o – Assumed overall heat transfer coefficient (W/m^{2}K).

(d) Calculation of the actual overall heat transfer coefficient (U_{Tx})

Overall heat transfer coefficient is characterized by coefficients of internal and external convection coefficients for the hot and cold fluids (Rosa & Júnior, 2017). Using Eq. (8), the actual overall heat transfer coefficient (U_x) for a single shell in a heat exchanger was calculated under the assumption of negligible heat resistance at the tube wall (Kern, 1965).

$$\frac{1}{U_x} = \frac{1}{h_t} + \frac{1}{h_s} + R_f \quad (8)$$

where R_f - the fouling factor, h_t - the convective heat transfer coefficient for the tube side (W/m^{2}K), and h_s – the convective heat transfer coefficient for the shell side (W/m^{2}K).

The actual overall heat transfer coefficient for the multi-shell heat exchanger (U_{Tx}) was calculated using Eq. (9).

$$U_{Tx} = U_x \times N_s \quad (9)$$

where N_s – the number of shells, x refers to section (heating, cooling, regeneration).

(e) Heat exchanger design margins

Margins are considered when designing heat exchangers to compensate for fouling, variable process or ambient conditions, and the risks of an exchanger that does not meet process requirements. Heat exchanger design margin refers to any heat transfer area that exceeds what is required by a clean heat exchanger to satisfy a specified duty (Bennett et al., 2007). The heat exchanger design margins were determined using over-surface design and over-design as given by Eq. (10) and (11), respectively (Bhatt & Javhar, 2014; Krishnan & Kumar, 2016).

$$\%Over - surface\ design = \left(\frac{U_{Tx} - U_0}{U_0}\right) \times 100 \quad (10)$$

$$\%Over - design = \left(\frac{A_H - A_{reg}}{A_{reg}}\right) \times 100 \quad (11)$$

where A_{req} is the required heat transfer area (m^2) determined using Eq. (12).

$$A_{reg} = \frac{\dot{q}}{U_{Tx}\Delta T_1} \quad (12)$$

(f) Estimation of the number of tubes

The number of tubes N_t was estimated using Eq. (13) (Bhatt & Javhar, 2014).

$$N_t = \frac{A_H}{A_0} \quad (13)$$

where A_o is the design heat transfer area.

(g) Determination of the number of tubes per pass and the actual number of tubes

The number of tubes per pass (N_{tp}) was determined from Eq. (14) (Shawabkeh, 2015).

$$N_{tp} = \frac{N_H}{N_p} \quad (14)$$

where N_p – the number of passes.

The actual number of tubes was determined from Eq. (15).

$$n = N_{tp} \times N_p \quad (15)$$

(h) Pressure drop calculations

According to Kakac et al. (2012) and Krishnan and Kumar (2016), tube – side pressure drop is a combination of pressure drop due to friction losses along the straight tube and the pressure drop due to the return loss. The pressure drop due to friction losses (ΔP_{ft}) and pressure drop due to return losses (ΔP_{rt}) were determined using Eq. (16) and (17), respectively.

$$\Delta P_{ft} = \frac{2 f_i L N_p \rho v^2}{D_i} \quad (16)$$

$$\Delta P_{rt} = 2N_P \rho v^2 \quad (17)$$

where: f_i is fanning friction factor, L is the length of the tube, Np is the number of passes, Di is the equivalent diameter of the tubes.

Shell-side pressure drop was the sum of friction pressure drop (ΔP_{fs}) determined by Eq. (18) (Yousufuddin, 2018) and the return pressure drop (ΔP_{rs}) determined by Eq. (19).

$$\Delta P_{fs} = \frac{f_0 G_m^2 (N_b + 1) D_i}{2\rho D_e \emptyset_s} \quad (18)$$

$$\Delta P_{rs} = 2(N_b + 1)\rho v^2 \quad (19)$$

where: G_m is the mass velocity of the shell-side fluid, (Nb +1) is the number of crosses, f_o is the shell side friction factor, D_i is the inside shell diameter, D_e is equivalent shell diameter, Φ_s is the viscosity correction factor for shell side.

2.1.3. Design of holding tubes

The product is held in the holding tubes for a specific amount of time and at a specific flow rate (Kanade & Subramani, 2014). The length of the holding tube was determined using the criteria outlined in Kanade and Subramani (2014) and calculated using Eq. (20).

$$Holding\ tube\ length = HT_{min} \times v_{max} \quad (20)$$

where HT_{min} – the minimum holding time (s) and V_{max} - the maximum velocity of flow in the holding tube.

2.1.4. Analysis of flow and sizing of the pumps

Electric power (P_{pump}) required by the motor to run the pump was determined using Eq. (21) (Oyedokun et al., 2017).

$$P_{pump} = \frac{W_P \times \dot{m}}{\eta_P - \eta_m} \quad (21)$$

where m – mass flow rate (kg/s), η_p and η_m - pump and motor efficiency, respectively, W_p – the pump hydraulic energy was determined using the Bernoulli Eq. (22).

$$W_P = \frac{(P_2 - P_1)}{\rho} + \frac{(U_2^2 - U_1^2)}{2} + g(Z_2 - Z_1) + E_f \quad (22)$$

where: P_1, P_2 – Pressure at the inlet side of the pump and outlet side respectively; U_1, U_2 – Mean velocity of flow on the inlet and outlet side of pump respectively; Z_1, Z_2 – Suction and elevation heads respectively; E_f - Friction losses along the path of flow.

2.1.5. Sizing of water heater

The size of the heater depends on the volume of water to be heated, temperature difference and the heating time. The heat load (P_h) required to rise the temperature of water per hour was calculated by Eq. (23).

$$P_h = \frac{4V_w \times \Delta T_w}{3412} \quad (23)$$

where V_m – Volume of water heated (L), ΔT_w – Rise in temperature of water (°C).

The time (hr) required to heat the water was determined using Eq. (24).

$$Time = \frac{P_h}{P_r} \quad (24)$$

where P_r – Heater power rating (kW).

2.2. Construction of the continuous pasteurizer

Using the equations in section 2.1, the size of every component in Fig. 1 was determined and engineering drawings developed. The drawings served as a guide in the fabrication of the pasteurizer. Corrosion resistance, cleanability, mechanical strength and weldability were key considerations when selecting materials for the parts responsible for holding and transferring the food, such as tanks and pipes. Thermal conductivity was also important in the selection of materials for heat exchanger construction.

2.3. Performance evaluation of continuous pasteurizer

Temperature and time are critical parameters that must be controlled effectively during pasteurization. The water must be at a higher temperature than the product in order for effective heat transfer between the hot water and the product. Estimating the time required for the water temperature to rise is critical in deter-mining the best time to turn on the pasteurization machine. The performance of the pasteurizer was evaluated by determining the maximum hot water temperature attainable, maximum hot water temperature attainable, product pasteurization temperature and throughput at various pumping speeds of the product.

2.3.1. Determination of maximum hot water temperature attainable

The hot water tank was filled to full capacity (65 L). The heaters and the hot water pump were turned on, with the pump set to its maximum speed (3000 rpm). The temperature of the water entering the heating section was monitored from the control panel until a maximum constant temperature was attained and recorded. The procedure was repeated three times.

2.3.2. Optimization of product flow rate for effective pasteurization

Using a variable frequency drive (Schneider Electric Model: ATV312H075M2) water used to simulate a low–viscous juice was pumped at speeds motor speeds of 180, 300, 420, 540, 660, 780, and 900 rpm and the pasteurization temperature attained determined. The hot water pump speed was kept at maximum (3000 rpm). The procedure was carried out in triplicate. A graph of pasteurization temperature versus product pump speed was plotted.

2.3.3. *Regression modelling approach to determine effect of product pump speeds on the throughput capacity and pasteurization temperature of continuous pasteurizer*

The throughput capacity and pasteurization temperature were assessed at the product pump speeds of 228, 252, 288, 354, 372, 384, 444, and 474 rpm. The selected speeds were within the optimal range for effective pasteurization using the continuous pasteurizer. All experiments were carried out while the hot water pump was running at maximum speed of 3000 rpm. Throughput capacity refers to the amount of fluid that passes through the system per unit time. The time required to process 20 L of product at each speed was measured and recorded using a stopwatch. Also, the pasteurization temperature was read from the control panel and recorded. Each experiment was done in triplicate for accurate results and then mean values were used. The throughput at each speed was calculated using Eq. (25).

$$Throughput = \frac{A_p}{T_p} \quad (25)$$

where A_p – Amount of product processed (L) and T_p – Time taken to process the product (hr)

Four regression models were fitted to the throughput capacity and pasteurization temperature curves so as to determine the best model for describing the pasteurizer machine behavior at different product pump speeds. The models are shown in Table 1. To demonstrate the validity of the fitted regression model, the throughput capacity and pasteurization temperature values obtained from the fitted models were compared with experimentally obtained values at speeds of 270, 330, 408, and 450 rpm.

Table 1. Regression models selected for this study.

Model No.	Regression model name	Model equation
1	Linear model	y = mx + c
2	Exponential model	y = a exp (bx)
3	Logarithmic model	y = a In(x) + b
4	Quadratic polynomial	$y = a x^2 + bx + c$

a, b, c, and m are coefficients and constants; y – Dependent variable (Throughput capacity or pasteurization temperature); x - product pump speed (rpm).

2.3.4. *Effect of variation in product pumping rate on the regeneration efficiency (RE)*

The RE was assessed at speeds within the optimal range for effective pasteurization using the continuous pasteurizer. Regeneration efficiency defines the relationship between the amount of heat supplied by the regeneration to the total heat load without regeneration (Chaudhary & Chaudhari, 2015). For all experiments, the hot water pump was kept at 3000 rpm. At product pump speed of 228 rpm, the inlet temperature for raw product (T_a) entering the regeneration section, the outlet temperature of the raw product (T_b) leaving the regeneration section, and the inlet temperature (T_c) for the hot product entering the shell-side of the regeneration section were detected by the temperature sensors and read off from the control panel. This experiment is done in triplicate. Regeneration efficiency (RE) was determined using Eq. (26). The procedure was repeated for product pump speeds of 288, 354, and 384 rpm and the corresponding regeneration efficiencies determined.

$$RE = \frac{T_b - T_a}{T_c - T_a} \times 100 \quad (26)$$

where: T_a is the inlet temperature of raw product (°C), T_b the outlet temperature of raw product leaving the regeneration section (°C), T_c the inlet temperature for the hot product to the regeneration section (°C).

2.4. *Statistical analysis*

To evaluate the model constants, the GNG nonlinear regression analysis was performed using the Microsoft Excel 2019 in-built Solver tool. Nonlinear regression was done on assumption that the model adequately represented the data. The quality of the model to predict the throughput capacity and pasteurization temperature was assessed based on the coefficient of determination (R^2), Standard Error Estimate (SEE), and Root Mean Square Error (RSME). The higher the R^2 value and lower SEE and RMSE values, the better the quality of model fitness to the experimental data (Borah & Hazarika, 2017; Malaikritsanachalee et al., 2018). The adequacy of the model was assessed using both ANOVA and regression analysis at $p < 0.05$ (Igboayaka et al., 2019). The standard residual error was used to evaluate the accuracy of the model to predict the observed values. The smaller the standard residual error, the better a regression model fits a dataset.

The RE was calculated as a percentage in MS Excel 2019. The data collected was first checked for normality by plotting the residual plots. The residual plots produced were normally distributed about the mean, with homogeneous variances, which meets the assumptions of analysis of variance (ANOVA). The variation of RE with product pump speed was analyzed using a one-way ANOVA ($p < 0.05$). The statistical calculations were carried out using the statistical program GenStat 14th Edition. MS Excel 2019 was used to create all graphs.

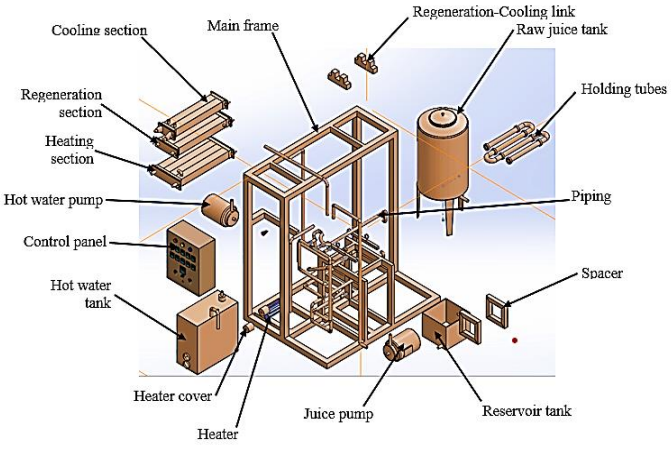

Fig. 1. The exploded view of the continuous pasteurizer.

Table 2. Heat exchanger design data.

Parameter	Units	Value			Reference Equation
		Heating section	Regeneration section	Cooling section	
The ratio of outlet temperature gap to inlet temperature (G)	-	0.04[§]	0.08[§]	0.44[§]	Eq. 2
Heat load (q)	kJ	14.33	12.22	3.39	Eq. 3
Thermal effectiveness (P)	-	0.76	0.62	0.36	Eq. 5
Heat capacity (P)	-	0.26	0.7	0.56	Eq. 6
Correction factor (F)	-	0.99[*†]	0.97[**†]	0.98[***†]	-
LMTD (ΔT_l)	°C	23.02	31.7	17.7	Eq. 4
Heating transfer area (A_H)	m^2	0.73	0.75	0.52	Eq. 7
Actual overall heat transfer coefficient for a single shell (U_x)	W/m^2K	238.5	182.1	205.8	Eq. 8
Actual overall heat transfer coefficient (U_{Tx})	W/m^2K	954	546.3	411.8	Eq. 9
Over-surface design	%	12.2[‡]	7.12[‡]	11.2[‡]	Eq. 10
Required heat transfer area (A_{req})	m^2	0.65	0.73	0.47	Eq. 12
Over-design	%	12.3	2.7	10.6	Eq. 11
Estimated number of tubes (N_t)	-	12	12	8	Eq. 13
Number of tube per pass (N_{tp})	-	2	2	2	Eq. 14
Actual number of tubes (n)	-	16	12	8	Eq. 15
Tube-side pressure drop	kPa	4.63[ǂ]	3.97[ǂ]	12.32[ǂ]	Eq. 16, 17
Shell-side pressure drop	kPa	0.102[†]	0.745[†]	0.273[†]	Eq. 18, 19

[*] Based on correction factor chart for 4-8 shell and tube heat exchanger (STHE) (Nitsche & Gbadamosi, 2016); [**] Based on correction factor chart for 3-6 STHE (Nitsche & Gbadamosi, 2016); [***] Based on correction factor chart for 2-4 STHE (Nitsche & Gbadamosi, 2016); [§] Acceptable for temperature approach (Vengateson, 2010); [†] Acceptable (Gulyani, 2000); [‡] Acceptable (Bhatt & Javhar, 2014; Krishnan & Kumar, 2016); [ǂ] Acceptable (Bhatt & Javhar, 2014; Kern, 1965); [†] Acceptable (Bhatt & Javhar, 2014; Kern, 1965).

Table 3. Statistical results obtained from selected regression models for throughput capacity and pasteurization temperature.

Parameter	Regression model name	Model constants and coefficients	SEE	R^2	RMSE
Throughput Capacity (L/h)	Linear model	m = 1.095, c = 435.721	31.3994	0.9090	28.5210
	Exponential model	a = 513.645, b = 0.001	33.4151	0.8930	30.9396
	Logarithmic model	a = 372.367, b = -1351.327	**26.6401**	**0.9364**	**23.8413**
	Quadratic polynomial	a = -0.003, b = 2.945, c = 138.967	26.2266	0.9349	24.3074
Pasteurization temperature (°C)	Linear model	m = -0.0174, c = 91.8793	0.2691	0.9736	0.2362
	Exponential model	a = 92.0792, b = -0.0002	0.2754	0.9723	0.2419
	Logarithmic model	a = -5.7424, b = 119.2523	0.3824	0.9449	0.3411
	Quadratic polynomial	a = 0.0000, b = -0.0025, c = 89.4181	**0.2283**	**0.9811**	**0.1996**

a, b, c, and m are coefficients and constants

Table 4. Validation of the experimental and predicted values of throughput capacity and pasteurization temperature.

Parameter	Throughput Capacity (L/h)				Pasteurization temperature (°C)			
Product pump speed (rpm)	Experimental	Predicted	Residual Error	Standard Residual Error	Experimental	Predicted	Residual Error	Standard Residual Error
270	747.09	733.34	-1.219	-7.608	86.00	88.74	0.0173	0.0894
330	820.08	808.06	-8.698	-31.248	85.33	88.59	-0.0232	-0.0884
408	865.42	887.07	19.242	70.140	84.00	88.40	0.00075	0.0029
450	923.19	923.56	-9.325	-50.374	83.33	88.29	0.00525	0.0272

3. Results and Discussion

3.1. *Description and mode of operation of the continuous pasteurizer*

The continuous pasteurizer consists of three heat exchangers (heating, regeneration, and cooling), two tanks (juice and hot water tank), a control panel, two pumps (hot water pump and juice pump), a holding tube, heaters, reservoir, and several piping to allow material flow on both the hot and cold sides. These parts are all attached to the main frame (**Error! Reference source not found.**). The machine is powered by a three-phase electric power supply. The three heat exchangers work in a counter-current flow as it provides the highest rate of heat transfer, making it ideal for fluid heating and cooling (Adumene et al., 2016). Prior to pasteurization, the heating medium (water) is heated for a specified period of time. The hot water is then pumped through the heating section, allowing heat to be transferred to the juice during pasteurization. Raw juice is pumped from the juice tank to the regeneration section using a juice pump, where it is preheated with

hot juice. It then flows to the heating section, where it is further heated to a specified pasteurization temperature. The juice is then held at the same temperature in the holding tubes for a short period of time before being cooled in the regeneration and cooling section. Temperature sensors and controls are integrated into the machine to assist in monitoring and regulating heat supply from the heaters, thereby controlling the pasteurization process as well as managing electric energy consumption.

3.2. Design of machine components

The juice tank diameter and height were determined as 0.44 m and 0.66m, respectively, using Eq. (1) considering that height and internal diameter were related as h=1.5 d (Hall, 2012). The results for the three heat exchangers were obtained by evaluating the various inlets and outlets temperatures, and flow parameters. Table 2 shows the design parameters for the heating, regeneration, and cooling section heat exchangers. Considering average residence time for the pineapple juice at the pasteurization temperature of 88°C as 15 sec (Widiatmo & Hendrarsakti, 2018), the length of the holding tube was calculated using Eq. (20) as 3 m. Pump hydraulic energy for the juice pump was calculated using Eq. (22) as 108.025 J/kg. Assuming the pump and motor efficiency of 70% and 60% respectively, the electric power (P_{pump}) required by the motor to run the juice pump was calculated using Eq. (21) as 0.034 HP. Hence, a juice pump of 0.1 Hp was used since the required power is less than the actual pump potential. The heat load per hour required to heat 50L of water from 27 to 100°C was calculated using Eq. (23) as 4.28 kW. Using two heaters each rated at 6kW, the time required to heat the water was calculated using Eq. (24) as 21.4 min.

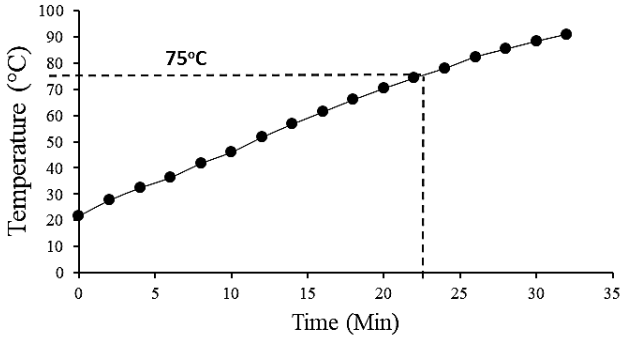

Fig. 2. Variation of water temperature with time during the initial heating process.

3.3. Performance evaluation of continuous pasteurizer

3.3.1. Determination of optimal hot water heating time prior to operation of the machine

Fig. 2 shows the relationship between hot water temperatures and heating time during the initial heating process. The water temperature steadily increased from 21.7 (room temperature) to 82.3°C in 26 minutes of heating at an average constant rate of 2.3 °C/minute. After 26 minutes of heating, the rate of change in temperature with time is observed to decrease to about 1.5 °C/minute, but drops further to 1.3 °C/minute after 30 minutes of heating. Fig. 2 shows that the heating process followed the theoretical heating curve for water in liquid phase with an initial steady rise at the start of heating but tending to flatten as it approaches the boiling point. The early decrease in the temperature change rate at only 82°C is attributable to the high elevation, which resulted in a reduction in boiling point for water. Makerere University, where the testing was conducted, is located at approximately 1240 m above sea level and has a boiling point of 95.5°C (Kiwana & Naluwagga, 2016).

The curve in Fig. 2 shows that the machine operator must initially run the heaters for a minimum of 23 minutes before turning on the machine for pasteurization. After 23 minutes of water heating, the water will be either at 75°C or other temperatures above 75°C worth heating the product to temperatures between 72°C and 88°C recommended for HTST processes (Bisig et al., 2019).

3.3.2. Optimization of product flow rate for effective pasteurization

The relationship between speeds and the achievable pasteurization temperature helps the operator to establish the optimal operating product pump speeds for effective pasteurization. Fig. 3 shows the pasteurization temperature achieved and maintained at different juice pump speeds. The corresponding average pasteurization temperature was found to be 87.57, 85.7, 80.0, 78.71, 76.29, 72.86, and 70.43°C for 180, 300, 420, 540, 660, 780, and 900 rpm, respectively. The findings indicate that high flow rates caused a reduction in pasteurization temperature. This is attributable to the reduced residence time for the product within the heat exchanger. The findings are consistent with those of Zhang et al. (2020). The findings show that all speed less than 792 rpm have the potential for use during the pasteurization as they result in temperatures higher than the minimum recommended pasteurization temperature of 72°C (for milk) under HTST conditions. According to Bisig et al. (2019), the recommended pasteurization temperatures for a HTST pasteurization process ranges between 72°C and 88°C. The optimal operating speed for pineapple juice was 200 rpm.

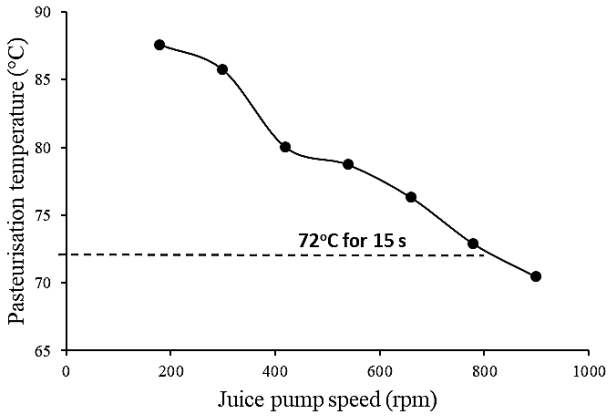

Fig. 3. A graph showing the speeds at which the product must be pumped for effective pasteurization.

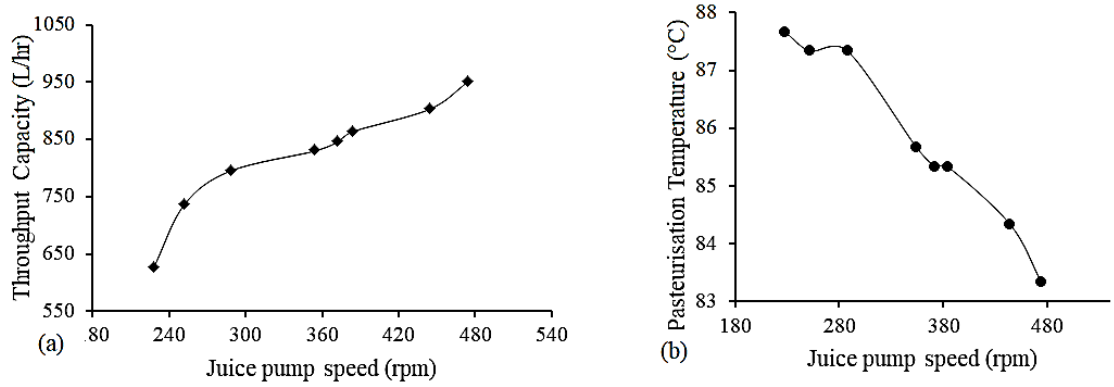

Fig. 4. Variation of (a) Throughput capacity with time (b) Pasteurization temperature with product pump speed.

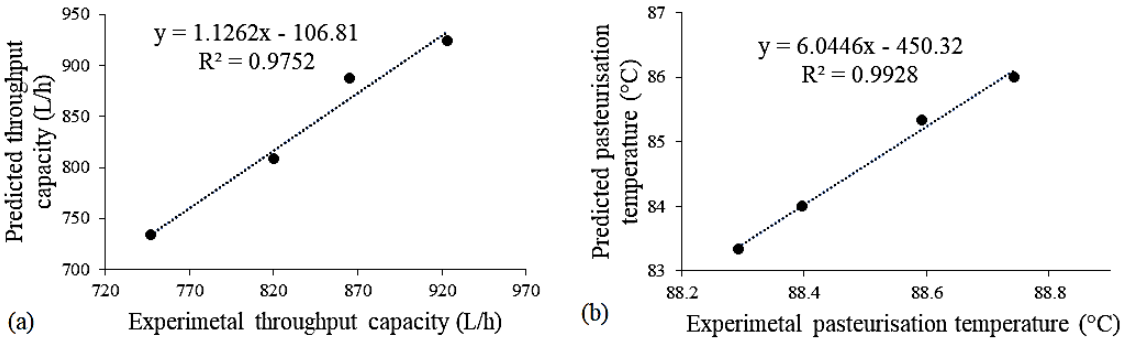

Fig. 5. Comparison of experimental and predicted values using the quadratic polynomial model for (a) Throughput capacity (b) Pasteurization temperature.

3.3.3. *Regression modelling approach to determine effect of product pump speeds on the throughput capacity and pasteurization temperature of continuous pasteurizer*

The increase in product pump speed resulted in a general increase in throughput capacity and reduction in pasteurization temperature as shown in **Error! Reference source not found.**a and b, respectively. From **Error! Reference source not found.**a, the pasteurizer has the potential to process over 600 L/h. This was high compared to 92-194 L/h found by Ahumuza et al. (2017) using a batch pasteurizer. The continuous nature of operation was responsible for the higher throughput capacity.

On fitting the experimental data to the four regression models, all models were considerably fit to predict the observed values for pasteurization temperature, except the logarithmic model. The model constants and coefficients for the fitted models are presented in Table 3. For the four regression models, the coefficient of determination (R^2) varied between 0.8930 and 0.9364, the Standard Error Estimate (SEE) varied between 26.2266 and 33.4151, while Root mean square error (RMSE) varied between 23.8413 and 30.9396 for the throughput capacity of the machine. The R^2 varied between 0.9449 and 0.9811, SEE varied between 0.2283 and 0.3824, while RMSE varied between 0.1996 and 0.3411 for the pasteurization temperature of the machine. The logarithmic model presented the highest R^2 and lowest SEE and RMSE values with 0.9364, 26.6401, and 23.8413, respectively for throughput capacity. The quadratic polynomial model presented the highest R^2 and lowest SEE and RMSE values with 0.9811, 0.2283, and 0.1996, respectively for pasteurization temperature. The logarithmic and quadratic polynomial models were best-fit models to predict the throughput capacity and pasteurization temperature, respectively (Table 3).

Table 4 shows the statistical values used in validating the experimental and predicted values of throughput capacity and pasteurization temperature with the logarithmic model and quadratic polynomial model, respectively. The range of the standard residual error for the throughput capacity of the continuous pasteurizer was found to range between -50.374 L/h and 70.140 L/h, while that of the pasteurization temperature was found to be -0.0884 to 0.0894°C (Table 4). The standard residual error for the throughput capacity and pasteurization temperature of the continuous pasteurizer was found to be close to zero. This indicates that the logarithmic model and the quadratic polynomial model give a good prediction for the throughput capacity and pasteurization temperature of the continuous pasteurizer respectively. The wide range of residual errors for the throughput model indicates that the model does not consistently fit all throughput capacity values. The results from the validation showed an R^2 value of 97.52% for the throughput capacity (**Error! Reference source not found.**a) and 99.28% for pasteurization

temperature (**Error! Reference source not found.**b). This implies that the quadratic regression model is in good agreement with the observed values with accuracy of more than 95% for both throughput capacity and pasteurization temperature. The models that describe the relationship between throughput capacity and pasteurization temperature with product pump speed are given in Eq. (26) and Eq. (27), respectively.

$$Y_c = 372.367\ In(X) - 1351.327 \quad (27)$$

$$Y_P = 0.00X^2 - 0.0025X + 89.4181 \quad (28)$$

where Y_c = Throughput capacity (L/h), Y_p = Pasteurization temperature (°C), X = product pump speed (rpm).

3.3.4. Effect of variation in product pumping rate on the regeneration efficiency (RE)

The regeneration efficiency varied between 48% and 54% for all operating product pump speeds used in the experiment. Analysis of variance indicated that there was no significant difference ($p < 0.05$) in the regeneration efficiencies at the different product pumping rates. The regeneration efficiency was highest at M288 with 53.91 ± 1.358%, followed by M228, M384, and M354 in that order at 51.92 ± 4.554%, 50.26 ± 2.909%, and 48.17 ± 1.85%, respectively. The results indicate that on average, 50% of the heat energy gained during the heating phase is used to preheat the cold product before the actual heating phase.

4. Conclusion

A small-scale continuous pasteurizer was successfully designed and fabricated. The machine is equipped with an automated control unit that allows for the adjustment of pasteurizing temperatures, allowing it to be utilized for a wide range of food products with pasteurization temperatures ranging between 72°C to 88°C under HTST processing. With an initial heating time of 23 minutes, all product pump speeds less than 792 rpm can yield a regeneration efficiency of about 50% with a throughput capacity of about 600 L/h. The pasteurizer's performance is therefore promising for use with low-viscous food products.

This technology should be extended among small-to-medium-scale processors so as to augment production while also reducing overall energy requirements via its regeneration mechanism. This machine is suitable for low viscous products such as pineapple juice, passion fruit juice, and lemon juice. While a reasonable initial heating time was achieved, the performance of the pasteurizer can be enhanced by improved control of the heating process with the installation of a pressure relief valve.

Funding

This work was funded by the Eastern and Southern Africa Higher Education Centers of Excellence Project supported by World Bank MAPRONANO ACE, Makerere University (Project ID: P151847).

Acknowledgment

E. B thanks Mr. Simon Tumusiime for opening gateways to the development of this research. E. B. is grateful to Mr. Ambrose Ashababehebwa and Mr. Fred Ofamba, all technicians at Flash Point Engineers and Fabricators Ltd workshop, Mukono -Uganda for accepting to share your expertise during the execution of this research. The Management of the Food Technology and Business Incubation Center (FTBIC), Makerere University is deeply appreciated for offering space to have the continuous pasteurizer fully tested.

Conflict of interest

The authors declare no conflict of interest.

References

Adumene, S., Nwaoha, T. C., Ombor, G. P., & Abam, J. T. (2016). Design and off-design performance evaluation of heat exchanger in an offshore process configuration. *Open Access Library Journal, 3*, e2748. doi:https://doi.org/10.4236/oalib.1102748

Ahumuza, A., Nabututa, E., Kigozi, J., Zziwa, A., & Sempiira, E. (2017). Design, construction and performance evaluation of an automatic batch pasteurizer. *Journal of Advances in Food Science & Technology, 4*(4), 145-154.

Amit, S. K., Uddin, M. M., Rahman, R., Islam, S. M. R., & Khan, M. S. (2017). A review on mechanisms and commercial aspects of food preservation and processing. *Agriculture & Food Security, 6*(51), 1-22. doi:http://dx.doi.org/10.1186/s40066-017-0130-8

Ankwasa, P. (2018). *Factors Affecting Pineapple Production In Ntungamo District.* Makerere University, Retrieved from http://www.dissertations.mak.ac.ug/bitstream/handle/20.500.12281/5614/ankwasa-cobams-bqe.pdf?sequence=1&isAllowed=y

Baidhe, E., Kigozi, J., & Balimunsi, H. K. (2022). Visualization of temperature and flow behavior in a continuous pasteurizer using computation fluid dynamics. *Open Access Library Journal, 9*, e8888. doi:https://doi.org/10.4236/oalib.1108888

Bennett, C. A., Kistler, R. S., Lestina, T. G., & King, D. C. (2007). Improving heat exchanger designs. *Chemical Engineering Progress, 103*(4), 40-45.

Bhatt, D., & Javhar, P. M. (2014). Shell and tube heat exchanger performance analysis. *International Journal of Science and Research, 3*(9), 1872-1881.

Bisig, W., Jordan, K., Smithers, G., Narvhus, J., Farhang, B., Heggum, C., Farrok, C., Saylor, A., Tong, P., Dornom, H., Bourdichon, F., & Robertson, R. (2019). *The technology of pasteurisation and its effect on the microbiological and nutritional aspects of milk*. Brussels, Belgium: International Dairy Federation.

Borah, A., & Hazarika, K. (2017). Simulation and validation of a suitable model for thin layer drying of ginger rhizomes in an induced draft dryer. *International Journal of Green Energy, 14*(13), 1150-1155. doi:https://doi.org/10.1080/15435075.2017.1369418

Chaudhary, D. A., & Chaudhari, A. G. (2015). Performance evaluation of a plate type (HTST) milk pasteurizer. *Research Journal of Animal Husbandry and Dairy Science, 6*(2), 130-134. doi:https://doi.org/10.15740/HAS/RJAHDS/6.2/130-134

Chavhan, S. D., Gohel, N. S., & Jha, R. S. (2016). Thermal-hydraulic performance of elliptic shape staggered tube cross flow heat exchanger at 45° angle of attack. *International Journal of Current Engineering and Technology* (Special Issue-5 (June 2016)), 75-77.

Deloitte. (2016). *Uganda Economic Outlook 2016: The Story Behind the Numbers*. Retrieved from https://www2.deloitte.com/content/dam/Deloitte/ug/Documents/tax/Economic Outlook 2016 UG.pdf

Hall, S. (2012). *Rules of thumb for chemical engineers* (5th ed.): Butterworth-Heinemann.

Igboayaka, E. C., Ndukwu, M. C., & Ernest, I. C. (2019). A Modelling approach for determining the throughput capacity and energy

consumption of a cassava tuber shredder. *Journal of the Chinese Advanced Materials Society, 6*(4), 801-816. doi:https://doi.org/10.1080/22243682.2018.1555678

Kakac, S., Liu, H., & Pramuanjaroenkil, A. (2012). *Heat Exchangers: Selection, rating, and thermal design* (Third ed.): CRC Press Taylor & Francis Group.

Kanade, P., & Subramani, A. (2014). Hygienic design aspects of pasteuriser to assure effective pasteruisation of milk. *Journal of Hygienic Engineering and Design, 8*, 19-29.

Kern, D. Q. (1965). *Process Heat Transfer* (Internatioal Student ed.). Tokyo, Japan: McGraw-Hill International Book Company, Inc.

Kikulwe, E., Okurut, S., Ajambo, S., Nowakunda, K., Stoian, D., & Naziri, D. (2018). Postharvest losses and their determinants: A challenge to creating a sustainable cooking banana value chain in Uganda. *Sustainability, 10*(7), 2381. doi:https://doi.org/10.3390/su10072381

Kiwana, D., & Naluwagga, A. (2016). *SEEK: Fuel performance of faecal sludge briquettes in Kampala, Uganda*. Retrieved from https://www.eawag.ch/fileadmin/Domain1/Abteilungen/sandec/schwerpunkte/ewm/SEEK/pdfs/kiwana_fuel_briquettes_kampala.pdf

Krishnan, N. M. C., & Kumar, S. B. (2016). An over view on shell and tube heat exchanger. *International Journal of Engineering Science and Computing, 6*(10), 2632-2636.

Kughur, P. G., Iornenge, G. M., & Ityonongu, B. E. (2015). Effects of postharvest losses on selected fruits and vegetables among small-scale farmers in gboko local government area of Benue state, Nigeria. *International Journal of Innovation and Scientific Research, 19*(1), 201-208.

Kumari, P., & Kumar, S. (2018). A study on post-harvest losses and constraints in banana cultivation in Vaishali district (Bihar). *The Pharma Innovation Journal, 7*(6), 93-95.

Kuteesa, A., Kisaame, E. K., Barungi, J., & Ggoobi, R. (2018). *Public Expenditure Governance in Uganda's Agricultural Extension System (ACODE Policy Research Paper Series, No. 84, 2018, Issue 84)*. Retrieved from https://www.africaportal.org/documents/18043/Public_expenditure_gov_uganda.pdf

Lebele-Alawa, B. T., & Ohia, I. O. (2014). Influence of fouling on heat exchanger effectiveness in a polyethylene plant. *Energy and Power, 4*(2), 29-34. doi:https://doi.org/10.5923/j.ep.20140402.01

Malaikritsanachalee, P., Choosri, W., & Choosri, T. (2018). Study on kinetics of flow characteristics in hot air drying of pineapple. *Food Science and Biotechnology, 27*(4), 1047-1055. doi:https://doi.org/10.1007/s10068-018-0357-6

Marwa, V. (2021). Design a VAT milk pasteurizer in Tanzania. *Academic Journal of Engineering Studies, 1*(4), AES.000525.

Ninshaba, P. (2015). *Design and construction of a gas heated milk pasteuriser*. Busitema University, Busitema, Uganda

Oyedokun, O. A., Achara, N., Muhammed, S. U., & Ishaq, O. O. (2017). Design and simulation of solar powered water pumping system for irrigation purpose in Kaduna, Nigeria. *International Journal of Scientific Engineering and Technology, 6*(10), 342-346. doi:https://doi.org/10.5958/2277-1581.2017.00053.5

Qian, X., Lee, S. W., & Yang, Y. (2021). Heat transfer coefficient estimation and performance evaluation of shell and tube heat exchanger using flue gas. *Processes, 9*(6), 1-19. doi:https://doi.org/10.3390/pr9060939

Rahiel, H. A., Zenebe, A. K., Leake, G. W., & Gebremedhin, B. W. (2018). Assessment of production potential and post-harvest losses of fruits and vegetables in northern region of Ethiopia. *Agriculture & Food Security, 7*(29). doi:https://doi.org/10.1186/s40066-018-0181-5

Rosa, V. d. S., & Júnior, D. d. M. (2017). Design of heat transfer surfaces in agitated vessels. In S. M. S. Murshed & M. M. Lopes (Eds.), Heat Exchangers - Design, Experiment and Simulation (pp. 37-60): InterOpen. doi:10.5772/66729

Sarkar, S. (2015). Microbiological Considerations: Pasteurized Milk. *International Journal of Dairy Science, 10*(5), 206-218. doi:https://doi.org/10.3923/ijds.2015.206.218

Shawabkeh, R. A. (2015). *Steps for design of Heat Exchanger*: Springer.

Uganda Investment Authority. (n.d.). *The Compendium of Investment and Business Opportunities Volume 2 (Business Start-up Ideas)*. Uganda Investment Authority Retrieved from https://washington.mofa.go.ug/sites/default/files/Compendium-of-Investment-and-Business-Opportunities-Vol-2.pdf

Vengateson, U. (2010). Design of multiple shell and tube heat exchangers in series: E shell and F shell. *Chemical Engineering Research and Design, 88*, 725-736. doi:https://doi.org/10.1016/j.cherd.2009.10.005

Wakholi, C., Cho, B.-K., Mo, C., & Kim, M. S. (2015). Current state of postharvest fruit and vegetable management in East Africa. *Journal of Biosystems Engineering, 40*(3), 238-249. doi:https://doi.org/10.5307/jbe.2015.40.3.238

Widiatmo, J. S., & Hendrarsakti, J. (2018). *Process Control of Milk Pasteurization using Geothermal Brine with Proportional Controller*. Paper presented at the 43rd Workshop on Geothermal Reservoir Engineering, Stanford University, Stanford, California.

Yousufuddin, S. (2018). Heat transfer enhancement of a shell and tube heat exchanger with different baffle spacing arrangements. *Scholar Journal of Applied Sciences and Research, 1*(6), 1-7.

Zhang, L., Shi, Z., & Yuan, T. (2020). Study on the coupled heat transfer model based on groundwater advection and axial heat conduction for the double u-tube vertical borehole heat exchanger. *Sustainability, 12*, 7345. doi:https://doi.org/10.3390/su12187345